Investigating a double layer Vivaldi antenna design for fixed array field measurement

Majid Ostadrahimi

Department of Electrical and Computer Engineering,
University of Manitoba,
Winnipeg, MB R3T 2N2, Canada
E-mail: morahimi@ee.umanitoba.ca

Sima Noghanian*

Department of Electrical Engineering,
University of North Dakota,
Grand Forks, ND 58202-7165, USA
E-mail: sima@mail.und.edu
*Corresponding author

Lotfollah Shafai, Amer Zakaria, Cam Kaye and Joe LoVetri

Department of Electrical and Computer Engineering,
University of Manitoba,
Winnipeg, MB R3T 2N2, Canada
E-mail: shafai@ee.umanitoba.ca   E-mail: azakaria@ee.umanitoba.ca
E-mail: cjkaye@ee.umanitoba.ca   E-mail: lovetri@ee.umanitoba.ca

Abstract: Vivaldi antenna is widely known as a broadband antenna. In this paper, we investigate a modified Vivaldi antenna with improved cross polarisation working in the ultra-wideband (UWB) frequency range (3.1–10.6 GHz) to be used as multiple probes for microwave tomography system. Our study includes investigation of radiation characteristics of the antenna, antenna design steps, fabrication sensitivity effects on the antenna performance and proposing and implementing a twenty-four antenna element system for fast data acquisition, including a novel method for frequency selection in microwave tomography applications. We also studied the fidelity parameter of the antennas inside the twenty-four element setup. The mutual coupling of adjacent elements, in spite of close proximity, is less than –17dB and fidelity variations for the antennas located in front of transmitter are less than 10%.

Keywords: microwave imaging; MI; microwave tomography; MWT; Vivaldi antenna; ultra wideband; UWB; polarisation; mutual coupling; multi-static near field measurement.

Biographical notes: Majid Ostadrahimi received his BSc and MSc in Electrical Engineering from Sharif University of Technology and Iran University of Science and Technology, Tehran, Iran, in 2003 and 2006, respectively. Currently he is pursuing his PhD in Electrical and Computer Engineering at the University of Manitoba, Manitoba, Canada. His research interests are microwave imaging especially from the antenna and measurement point of view, dielectric measurement and near field measurement techniques.

Sima Noghanian received her MSc and PhD, both in Electrical Engineering, from University of Manitoba, Winnipeg, Canada in 1996 and 2001, respectively. She was an Assistant Professor of the Electrical Engineering Department of Sharif University of Technology in 2002–2003, and an Assistant Professor with the Electrical and Computer Engineering Department of University of Manitoba in 2003–2008. Currently she is an Assistant Professor with the Electrical Engineering Department of University of North Dakota. Her research interests include antenna design and modelling, wireless channel modelling, ultra-wideband antennas and microwave imaging. She is a senior member of IEEE.

Lotfollah Shafai completed his BSc at the University of Tehran in 1963 and MSc and PhD in the Faculty of Applied Sciences and Engineering, University of Toronto, in 1966 and 1969. In November 1969, he joined the Department of Electrical and Computer Engineering, University of Manitoba as a Lecturer, became an Assistant Professor in 1970, Associate Professor in 1973, and Professor in 1979. He is currently, a Distinguished Professor and holds a Canada Research Chair in Applied Electromangetics. He is a Life Fellow of IEEE, a Life Fellow of Royal Society of Canada, a Fellow of Canadian Engineering Academy and a Fellow of Engineering Institute of Canada.

Amer Zakaria received his BSc in Electrical Engineering (Summa cum laude) from the American University of Sharjah, Sharjah, United Arab Emirates, in 2005 and his MSc in Microwave Engineering (with high distinction) from Munich University of Technology, Munich, Germany in 2007. Currently, he is pursuing his PhD in Electrical Engineering at the University of Manitoba, Winnipeg, Canada. His current research interests are in the areas of computational electromagnetics and inverse problems.

Cameron Kaye received his BSc in Computer Engineering in 2005 and his MSc in Electrical Engineering in 2009, both from the University of Manitoba, Winnipeg, MB, Canada. He is currently a member of the Faculty of Medicine, University of Manitoba, where he is also with the Microwave Imaging Research Group, Department of Electrical and Computer Engineering, and is engaged specifically in the development of microwave tomography prototypes. His research interests include calibration techniques for imaging within resonant enclosures.

Joe LoVetri received his PhD in Electrical Engineering from the University of Ottawa, ON, Canada, in 1991. From 1991 to 1999, he was an Associate Professor in the Department of Electrical and Computer Engineering, University of Western Ontario, Canada. He is currently a Professor in the Department of Electrical and Computer Engineering at the University of Manitoba, Winnipeg, Canada. His main research interests are in computational electromagnetics, modelling of EMC problems, microwave tomography, biomedical imaging, and inverse problems.

1 Introduction

Electromagnetic field measurement has been of interest for many years. The accuracy and design of a field measurement setup depends on its application. Basically, there are two major categories in field measurement methods: mono-static and multi-static. In a mono-static system, such as mono-static ground penetrating radar (GPR), an individual antenna works as a transceiver. In a multi-static system, one antenna works as the transmitter and other antennas collect the data. The latter category may be implemented by a single transmitter and single receiver, or multiple transmitters and multiple receivers. Microwave imaging (MI) setups for biomedical applications using both methods have been recently presented (Semenov, 2009).

MI has been shown to be a promising technology for biological imaging (Meaney et al., 2000, 2007; Fear et al., 2002; Winters et al., 2008; Semenov, 2009; Klemm et al., 2009). In this application, the unknown object is illuminated by microwave energy and scattered fields are collected to reconstruct the image. To do the measurement at different points using mono-static imaging setups, it is necessary for the antenna to move relative to the target object. However, moving the antenna introduces stress on the cables and connectors that causes measurement error. One solution for reducing these errors is to move the object under the test, instead of the antenna. This solution is not easily applicable in the case of an MI clinical system, when the object is a patient. Another disadvantage of a mono-static measurement system is the long measurement time. In a clinical system, a patient's movement during the test can cause inaccuracies in the measurements and image artefact.

Various antennas have been reported to be used for the mono-static MI. A resistively loaded double-ridged pyramidal horn is reported by Li et al. (2004). This antenna features a very compact size and is intended to be immersed in oil. There is no report on the cross polarisation characteristic of this antenna, but it features a very good fidelity for pulse transmission. A modified horn from the Tera-X company was also reported (Winters et al., 2008). Resistive Wu-King monopole (Fear et al., 2003; Sill and Fear, 2005) is another antenna being used for mono-static measurement. In spite of being very compact in size, this antenna has low sensitivity due to its omni-directional pattern, and low efficiency due to its resistive behaviour.

Recently, cross Vivaldi antenna (Zhang et al., 2009) has also been reported to be used in mono-static MI measurements. Although this antenna has a directional pattern, its polarisation purity was not reported.

In a multi-static tomography setup, as mentioned, the receiver and transmitter antennas are not the same. By using multiple antennas, the acquisition time decreases significantly.

In a widely known experiment reported by Geffrin et al. (2005), one broadband double ridged horn antenna was used as a fixed transmitter and a similar antenna was utilised as the receiver. The object was placed at the centre, while the transmitter and receiver encircled it at the distance of 1.67 m. The receiver circularly swept the object in 1° steps.

To avoid errors caused by the mechanical movement of cables, the transmitted and received signals in the cables were at very low frequency (20 MHz). This signal was then down/up-converted to the desired frequencies using a mixer connected to the antenna. The broadband nature of the antennas allowed the measurements to be performed at a wide frequency range of 2–18 GHz. A three dimensional version of this setup was recently reported (Geffrin, and Sabouroux, 2009). Although these wideband measurements were reasonably accurate, they required long acquisition times, which is unsuitable for clinical applications.

Multiple antennas have also been used in some early MI setups. In an experiment by Meaney et al. (1995), four waveguides served as transmitters and four monopoles as receivers, located close to the object. Each antenna was followed by a switch which activated the transmitter and receiver antennas. Monopole antennas used in this experiment were constructed by removing a quarter wavelength of the insulating shield from semi-rigid coaxial cables and exposing their inner conductors. To increase the bandwidth, monopoles were suspended in saline solution and to acquire more data points, they were physically rotated. In the next version of this system reported by Meaney et al. (2000), instead of using monopoles and waveguides simultaneously, only monopoles were used and their quantity increased from 4–32. One of them would serve as transmitter while the rest were receivers.

In this paper, we investigate a modified double layer Vivaldi Antenna (DLVA) to be used in a multi-static tomography system with fast acquisition time.

The antennas are designed such that mutual coupling is minimised in close proximity with other DLVAs. The reason for choosing DLVA, is that they are intrinsically broadband, and can provide a pure polarisation for MI measurements. Their directive pattern, with an average gain of 7 dBi, can increase the sensitivity of the system, by concentrating the power in one direction. Another advantage to the directive pattern is presenting a wide beam in one plane and narrow beam in the other which is very useful for illuminating a 2D slice of the object in a tomography system.

Single layer Vivaldi antenna in a circular array was suggested for MI measurements (Abbosh et al., 2006). The level of cross-polarisation (X-pol) of this antenna can be improved by adding another layer. This leads to better polarisation purity (Langley et al., 1993). Our double layer design has improved the X-pol by at least 10 dB (Ostadrahimi et al., 2009).

We have studied the fabrication sensitivity of DLVA and found that even a small misalignment in the fabrication, significantly deteriorates the X-pol, especially in the *E*-plane. Considering the fabrication sensitivity and X-pol improvement, we developed a fixed array of twenty-four antenna elements for a tomography system. In this setup the antennas are located in the air, (unlike previously reported setups that employ a lossy solution). Our measurements show the mutual coupling to be less than −17 dB and it is expected that the mutual coupling level will be lower in a lossy matching medium. The proposed system is capable of switching the transmitter and it can illuminate the object through each of twenty-four antennas at 15° steps. At each step, the other 23 antennas act as receivers. They can provide 24 × 23 data measurement points, without any need of physically moving the antennas, or the object under test. By rotating the object, it is possible to collect more data points for different applications. Images of different objects have been reconstructed successfully using the proposed system (Gilmore et al., 2009a, 2009b).

2   Antenna configuration, design steps

2.1   Antenna description

DLVA consists of two major parts, feed line and the radiation flares. The shape of the flares follow an elliptical configuration as it is one of the optimum curvatures (Abbosh et al., 2006). Since the antenna is fabricated on two substrates, the excitation can be provided by a stripline transmission line, which is tapered gradually to the radiation flares. Because of the gradual tapering from the unbalanced stripline feed to balanced radiation flares, there is no need to use a balun for this structure.

All simulations are done by finite element method (Ansoft HFSS, 2009).

2.2   Design steps

The antenna geometry is shown in Figure 1. The design procedure is as follows:

1   Substrate: We chose Arlon-Diclad 527 substrate with relative permittivity of $\varepsilon_r = 2.40 - 2.65$ and loss tangent of $\tan\delta = 0.0022$. Depending on the availability and the size of the stripline connector, choices of substrate thickness are limited. We used the thickness of $h = 0.0625$ inch.

Figure 1   The basic configuration of DLVA, (a) four constructive ellipses, (b) upper layer, (c) lower layer, (d) fabricated antenna including *H*- and *E*-planes and coordinate system (see online version for colours)
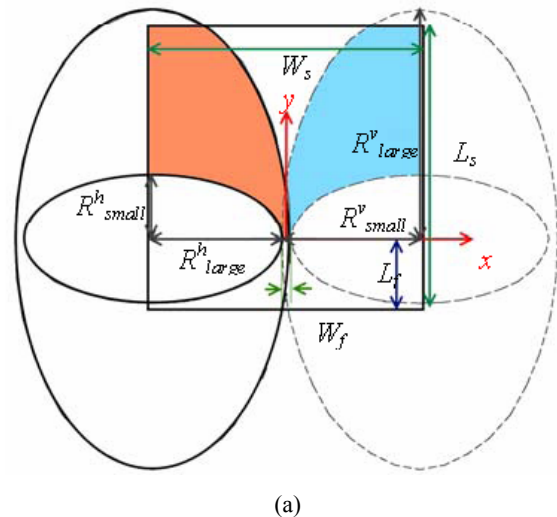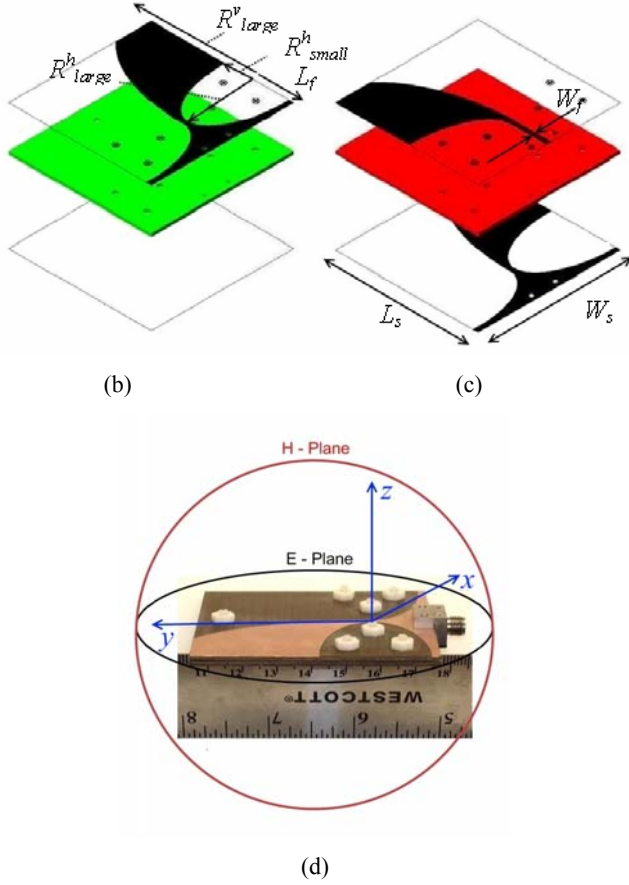

(a)

(b)   (c)

(d)

2 Antenna main dimensions: Theoretically, the upper frequency limit of a Vivaldi antenna is infinity. The lower frequency limit depends mainly on W_s that should be half of the effective wavelength (λ_{eff}) at the lowest frequency. The effective wavelength was calculated from (1) (Pozar, 1999).

$$\lambda_{eff} = \frac{\lambda_0}{\sqrt{\varepsilon_r}} = \frac{c}{f\sqrt{\varepsilon_r}}, W_s = \frac{\lambda_{eff}}{2} \qquad (1)$$

W_f, the feed line width, is calculated from the standard stripline equation (2) (Pozar, 1999).

$$x = \frac{30\pi}{\sqrt{\varepsilon_r}Z_0} - 0.441$$

$$\frac{W_f}{h} = \begin{cases} x & \sqrt{\varepsilon_r}Z_0 < 120 \\ 0.85 - \sqrt{0.6 - x} & \sqrt{\varepsilon_r}Z_0 > 120 \end{cases} \qquad (2)$$

The antenna length consists of feed (L_f) and radiation portions ($L_s - L_f$), which consists of three ellipses: one on the left side, and the other two on the right side, as shown in Figure 1. Smoother tapering of the radiation portion provides a smoother gain, but increases the size. Decreasing the feed portion causes a better impedance bandwidth; however, it deteriorates the gain flatness within the operating bandwidth. To find an optimum

point for the maximum bandwidth, minimum size and flat gain versus frequency, a parametric study was done. This optimisation of DLVA geometry was performed using a parametric sweep on radiation flare curves in terms of ratios of ellipses' radii. Then the impedance bandwidth and gain characteristic versus frequency were compared in Ansoft HFSS. Optimum values were calculated from (3).

$$L_s = W_s = 70mm, L_f = 18mm$$

$$R_{small}^v = \frac{W_s}{2}, \qquad \frac{R_{small}^h}{R_{large}^h} = 0.48$$

$$R_{large}^h = \frac{W_s - W_f}{2}, \qquad \frac{R_{large}^v}{R_{small}^v} = 1.67 \qquad (3)$$

3 Sandwiching: The two layers should be sandwiched. We used Nylon screws for this purpose, since their dielectric properties are very close to that of the substrate. The fabricated antenna is shown in Figure 1(d).

Figure 2 DLVA reflection coefficient, frequency step in simulation is 25.6 MHz and in measurement is 40 MHz (see online version for colours)
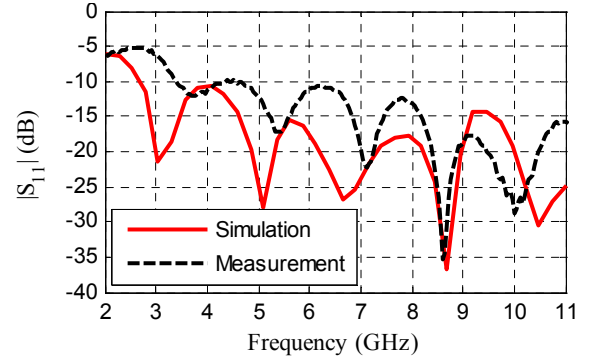

3 Measurement results and radiation behaviour

3.1 Impedance bandwidth and radiation pattern

The impedance bandwidth or reflection coefficient is shown in Figure 2. The impedance bandwidth covers the frequency band from 3.3 GHz to 10 GHz. There is a shift between the measurement and simulation, which is mainly due to fabrication error for mounting the connector and numerical computation error in simulation.

Radiation pattern: The *E*- ($x - y$) and *H*- ($z - y$) planes' radiation patterns are illustrated in Figure 1(d). For the pattern measurements (Figure 3), the anechoic chamber was calibrated by a reference horn antenna. The minimum sensitivity of the compact range measurement in our chamber is –30 dB, therefore, the X-pol results under –30 dB are not valid. The angular resolution of measurement is 1°. Figure 4 through Figure 10 show the measurement and simulation results. In these figures M, S, Co, and X stand for the measured, simulated, co-polarisation (Co-pol) level, and X-pol level, respectively.

Figure 3   DLVA antenna pattern measurements in anechoic chamber (see online version for colours)
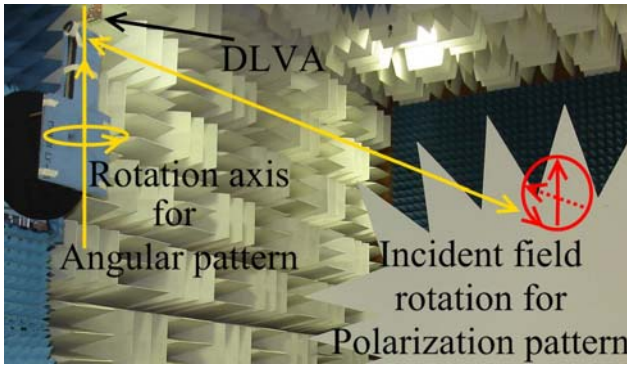
Figures 4 to Figure 6 compare the results for the *H*-plane at three frequencies, 3.7, 6.7 and 9.7 GHz, respectively. As expected, the pattern is wider in this plane. There is a good agreement between the simulation and measurement results at all frequencies.

Figure 7 to Figure 9 show the same parameter in the *E*-plane. The agreement between the simulation and measurement results, in Co-pol pattern, is very good, but measurement results of the X-pol do not follow the simulation results. To achieve further certainty of proper measurement results, we performed another kind of measurement which the receiver was constant and transmitter was revolving. To perform this measurement, DLVA was mounted once in the *E*-plane and then in *H*-plane, while the transmitter of anechoic chamber was revolving (Figure 3). The result of these measurements for the centre frequency of 6.7 GHz is shown in Figure 10. It can be seen that the X-pol level is –36 dB and it is symmetrically changing. This is consistent with the results of Figure 5 and Figure 8 from the normal pattern measurement. Similar results were observed at other frequencies.

Figure 4   Comparison of the simulated and measured Co- and X-pol gain patterns of the antennas at 3.7 GHz, *H*-plane (see online version for colours)
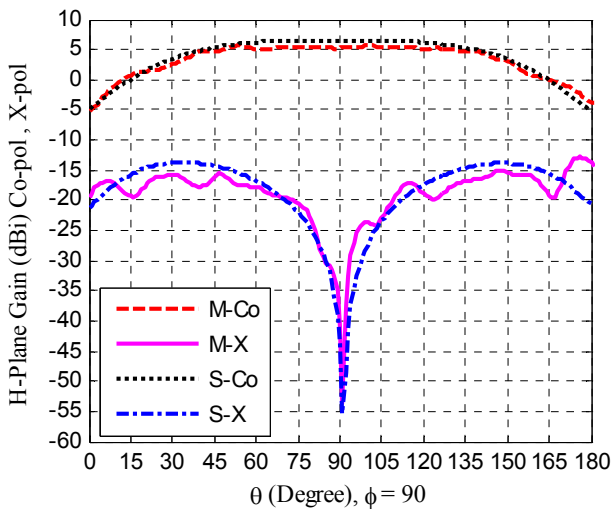

Figure 5   Comparison of the simulated and measured Co- and X-pol gain patterns of the antennas at 6.7 GHz, *H*-plane (see online version for colours)
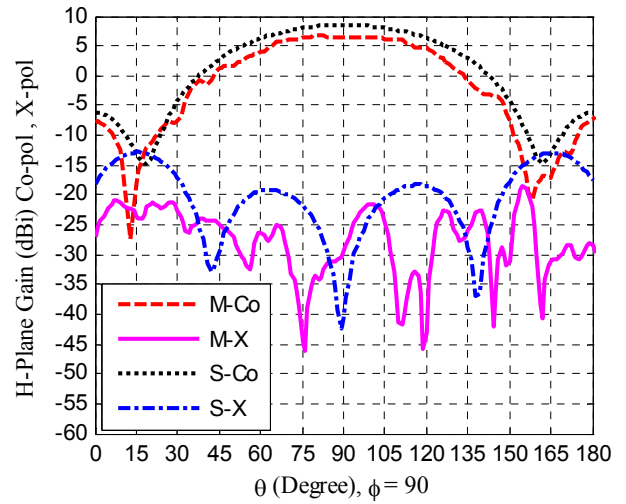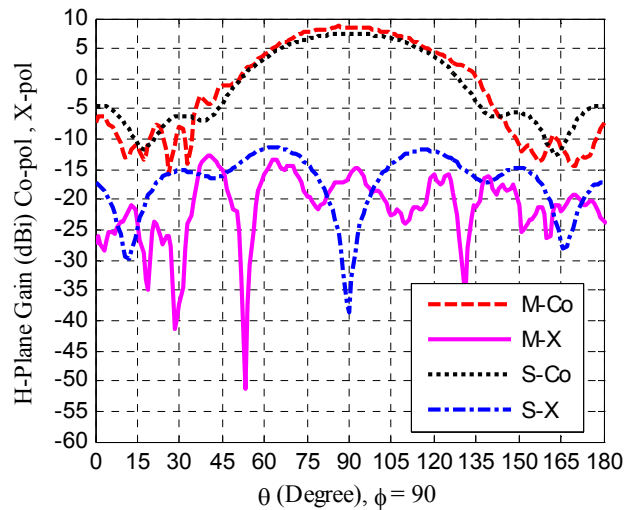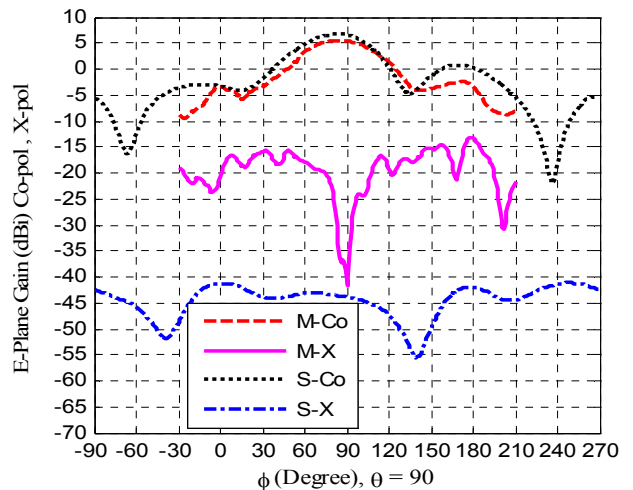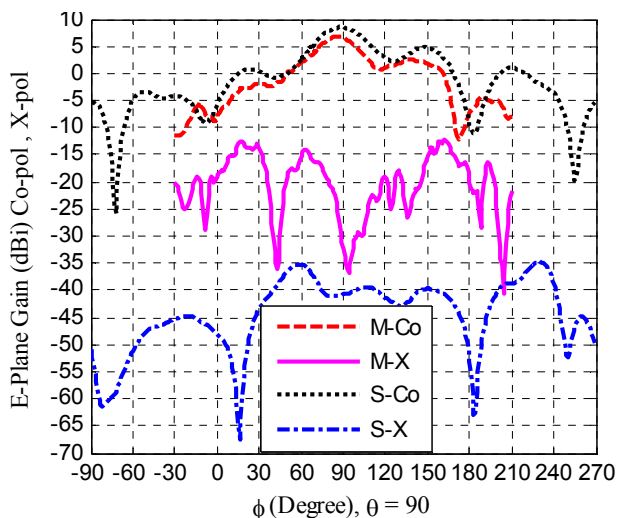

Figure 6   Comparison of the simulated and measured Co- and X-pol gain patterns of the antennas, at 9.7 GHz, *H*-plane (see online version for colours)

Figure 7   Comparison of the simulated and measured Co- and X-pol gain patterns of the antennas at 3.7 GHz, *E*-plane (see online version for colours)

Figure 8 Comparison of the simulated and measured Co- and X-pol gain patterns of the antennas at 6.7 GHz, *E*-plane (see online version for colours)

Figure 9 Comparison of the simulated and measured Co- and X-pol gain patterns of the antennas at 9.7 GHz, *E*-plane (see online version for colours)
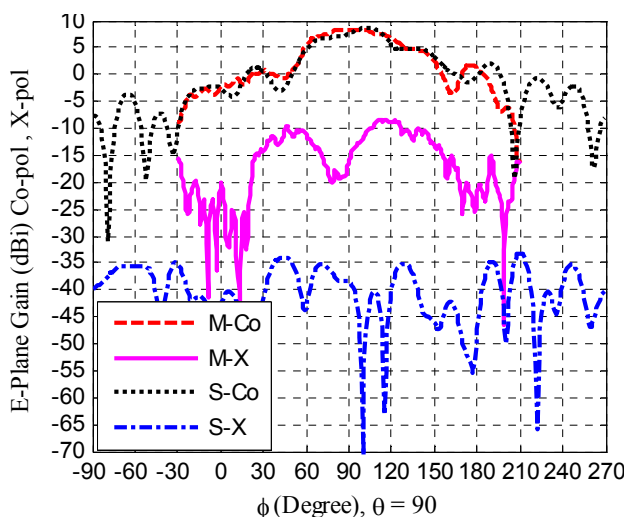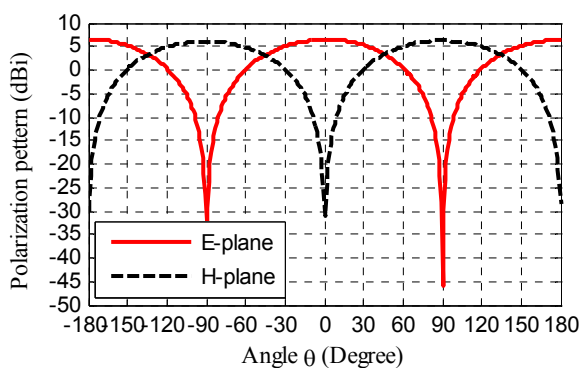

Figure 10 Polarisation patterns of the antenna at 6.7 GHz, measured as in Figure 3 (see online version for colours)

After validation of X-pol measurement by two methods, we studied fabrication sensitivity to investigate the source of error in the *E*-plane pattern.

3.2 *Fabrication sensitivity*

To study the sensitivity of the antenna performance to fabrication tolerances, we simulated three cases which are described in Table 1. In these cases, misalignments in horizontal and vertical axes are considered, which could happen in our fabrication process. Simulations show that this effect significantly deteriorates the *E*-plane X-pol level, but it hardly changes the X-pol level in the *H*-plane.

Table 1 Fabrication tolerances due to misalignment

Case	Description
1	Ideal alignment of upper and lower layers.
2	Misalignment of one layer in horizontal direction (x–y plane) by 0.5 mm.
3	Misalignment of one layer in vertical direction (z–y plane) by 1°.

Simulation results are shown in Figure 11 to Figure 13 at three frequencies within the bandwidth. As depicted in these figures, the *E*-plane X-pol level increased by at least 15 dB due to the fabrication errors.

Figure 11 Effect of fabrication error on simulated *E*-plane X-pol at 3.7 GHz (see online version for colours)
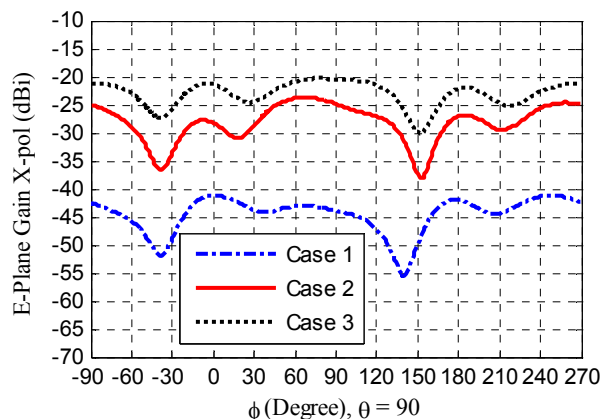

Figure 12 Effect of fabrication error on simulated *E*-plane X-pol at 6.7 GHz (see online version for colours)
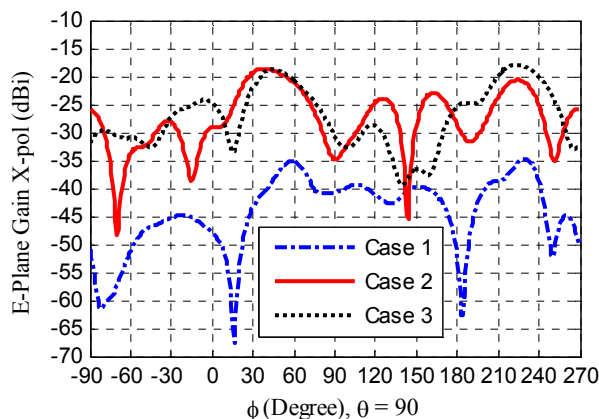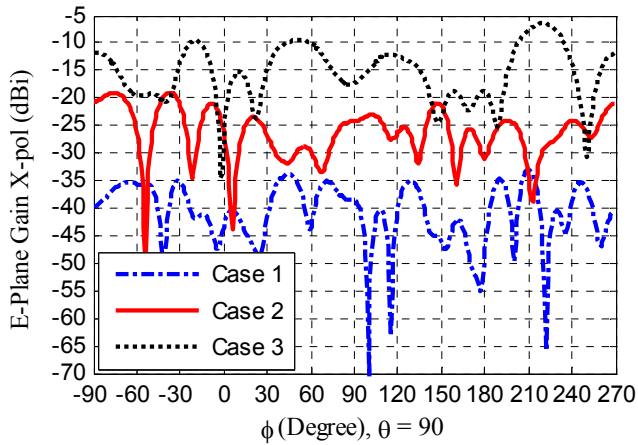
Figure 13 Effect of fabrication error on simulated *E*-plane X-pol at 9.7 GHz (see online version for colours)

4   Proposed field measurement setup

The directive patterns and low X-pol level of the DLVA makes it a good candidate for a multi-static tomography setup. Twenty-four DLVAs were fabricated and mounted on a Plexiglas cylinder of 45 cm diameter with equal angular spacing of 15°. The antennas are connected to a 2 × 24 mechanical switch network (Agilent 87050A-K24) using coaxial cables of equal lengths. The network analyser (Agilent E-8363B) is directly connected to the switch network. This setup is shown in Figure 14. To illuminate the entire surface of the object, the DLVAs should be mounted vertically. In this situation, the wider beam of the antenna pattern is towards the object, while the narrower beam focuses the energy towards the illumination plane. The antennas were labelled from 1 to 24, as shown in Figure 14(b).

Figure 14 Measurement setup including 24 DLVA, (a) top view, (b) switch network and network analyser (see online version for colours)
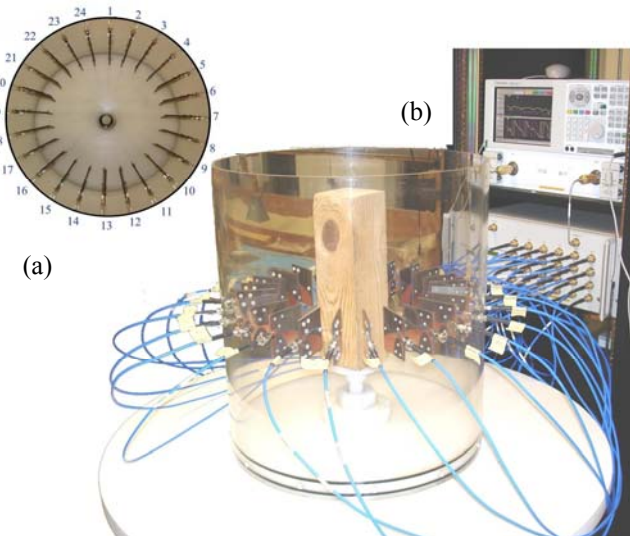
To study the mutual coupling of the antennas, we compared their performance alone and in the presence of the other antennas, while mounted in a Plexiglas chamber. For this experiment, we performed a full 2-port calibration, with port 1 as a reference and ports 2–23 as forward. We used HP 85033D 3.5 mm calibration kit which is valid up to 6 GHz. Therefore, there might be some calibration error at higher frequencies (more than 6 GHz). Figure 15 and Figure 16 show the reflection coefficients, for both phase and amplitude, of each DLVA in the air and in the presence of the other antennas. As indicated in these figures, the reflection coefficient is higher at some frequencies between 3 GHz–4.5 GHz. This change in the reflection coefficient indicates the loading effects due to the presence of the chamber and other antennas. It can also give an indication as to which working frequencies should be selected for the microwave tomography (MWT) operation. As mentioned by Gilmore et al. (2009b), the image reconstruction error is lower at frequencies where the reflection coefficient is invariant. One expects to improve this behaviour by filling the enclosure with a lossy solution. Figure 17 shows the transmission between antenna #1 and other antennas, which highlights the level of mutual coupling. As shown in this figure, the mutual coupling is less than –17 dB at frequencies higher than 4 GHz and there is a good isolation between elements at these frequencies.

Because of the directional pattern of the DLVA, we studied fidelity parameter as explained in Li et al. (2004), to measure how many receivers are uniformly illuminated by a transmitter. After a full 2-port calibration, the S_{n-1} for $n = 1–24$ are collected at 3059 sampling points within the frequency range of 3.3 to 10 GHz. By assuming a perfect calibration at all frequencies, the time domain equivalent pulse of this spectrum is reconstructed in Matlab. Cross-correlation of the time derivation of this pulse and the measured pulse at each receiver indicates the similarity of the pulse shape between different antennas.

Figure 15 Reflection coefficient amplitude of each antenna in presence of other 23 DLVA in the measurement system (see online version for colours)
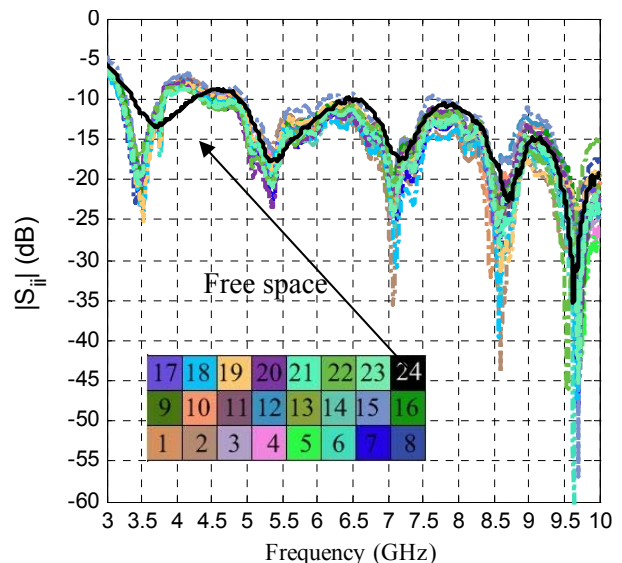
Figure 16 Reflection coefficient unwrapped phase of each antenna in presence of other 23 DLVA in the measurement system (see online version for colours)
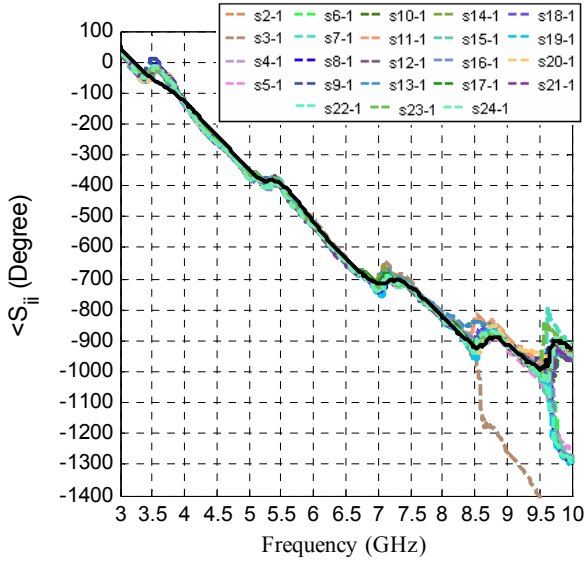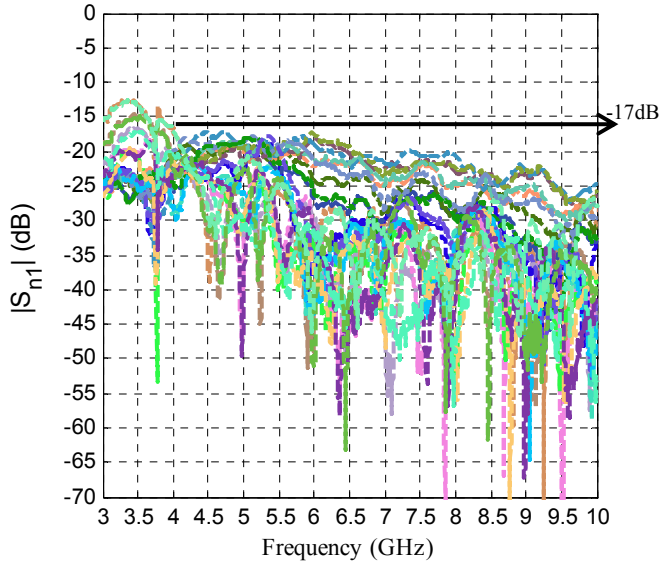

Figure 17 Amplitude of mutual couplings between antennas (see online version for colours)

Cross correlation of the *i*th antenna is calculated from (4):

$$F^i = \max_\tau \int_{-\infty}^{\infty} r(t-\tau) f^i(t) dt \qquad (4)$$

where, $f^i(t)$ is the received pulse at *i*th antenna and $r(t)$ is the time derivative of ideal transmitted pulse. This cross-correlation is then normalised to the energy of both the transmitted and received signals and is called 'fidelity' of each antenna. Our calculation shows when the antenna 1 is transmitter, the changes in fidelity of antennas 9 to 17 is less than 10%. Therefore by sending a pulse that covers the operating frequency range of 3.3 to 10 GHz, the nine antennas in front of the transmitter, will receive the expected pulse with less than 10% error. This shows a uniform illumination and good isolation between antennas.

5 Conclusions

A multi-antenna measurement setup of twenty-four DLVAs was presented. We explained the design procedure and radiation parameters of the DLVA, as well as investigating the sensitivity of the DLVA to fabrication error. This error directly affects the *E*-plane X-pol level. By measuring the fidelity, reflection coefficient and forward *S*-parameters we studied the mutual coupling and uniform illumination of the object under test. The proposed setup shows a good isolation between DLVAs, while their radiation characteristics remain unchanged, which is a distinct advantage for MWT applications. Also the variations in reflection coefficient indicate the optimum operating frequency for MWT. Results of reconstructed images using the proposed system are presented in Gilmore et al. (2009b).

References

Abbosh, A.M., Kan H.K. and Bialkowski, M.E. (2006) 'Compact ultra-wideband planar tapered slot antenna for use in a microwave imaging system', *Microwave Opt. Tech. Lett.*, No. 48, pp.2212–2216.

Ansoft HFSS a subsidiary of ANSYS Inc. (2009) Available at http://www.ansoft.com/products/hf/hfss/ (accessed on 17 July).

Fear, E.C., Hagness, S.C., Meaney, P.M., Okoniewski, M. and Stuchly, M.A. (2002) 'Enhancing breast tumor detection with near-field imaging', *IEEE Mic. Magazine*, Vol. 3, No. 1, pp.48–56.

Fear, E.C., Sill, J. and Stuchly, M.A. (2003) 'Experimental feasibility study of confocal microwave imaging for breast tumor detection', *IEEE Trans. on Mic. Theory and Tech.*, Vol. 51, No. 3, pp.887–892.

Geffrin, J., Sabouroux, P. and Eyraud, C. (2005) 'Free space experimental scattering database continuation experimental setup and measurement precision', *Institute of Physics Inverse Problems*, Issue 6, pp.117–130.

Geffrin, J.M. and Sabouroux, P. (2009) 'Continuing with the Fresnel database: experimental setup and improvements in 3D scattering measurements', *Inverse Problems*, Vol. 25, No. 2, pp.024001 (18pp).

Gilmore C., Mojabi, P., Zakaria, A., Ostadrahimi, M., Kaye, C., Noghanian, S., Shafai, L., Pistorius, S. and LoVetri, J. (2009a) 'An ultra-wideband microwave tomography system: preliminary results', Paper presented at *IEEE Engineering in Medicine and Biology Society (EMBS) Conf.*, 2–6 September, Minneapolis, USA.

Gilmore C., Mojabi, P., Zakaria, A., Ostadrahimi, M., Kaye, C., Noghanian, S., Shafai, L., Pistorius, S. and LoVetri, J. (2009b) 'A wideband microwave tomography system with a novel frequency selection procedure', Accepted for publication in *Biomedical Engineering, IEEE Transaction on.*

Klemm, M., Craddock, I.J., Leendertz, J.A., Preece, A. and Benjamin, R. (2009) 'Radar-based breast cancer detection using a hemispherical antenna array – experimental results', *Antennas and Propagation, IEEE Transactions on*, Vol. 57, No. 6, pp.1692–1704.

Langley, J.D.S., Hall, P.S. and Newham, P. (1993) 'Novel ultrawide-band Vivaldi antenna with low crosspolarisation', *Electronics Letters*, Vol. 29, No. 23, pp.2004–2005.

Li, X., Davis, S.K., Hagness, S.C., Van der Weide D.W. and Van Veen, B.D. (2004) 'Microwave imaging via space-time beamforming: experimental investigation of tumor detection in multilayer breast phantoms', *IEEE Trans. on Mic. Theory and Tech.*, Vol. 52, No. 8, pp.1856–1865.

Meaney, P.M., Fanning, M.W., Dun, L., Poplack, S.P. and Paulsen, K.D. (2000) 'A clinical prototype for active microwave imaging of the breast', *IEEE Trans. on Microwave Theory and Techniques*, Vol. 48, No. 11, pp.1841–1853.

Meaney, P.M., Fanning, M.W., Raynolds, T., Fox, C.J., Fang, Q., Kogel, C.A., Poplack, S.P. and Paulsen, K.D. (2007) 'Initial clinical experience with microwave breast imaging in women with normal mammography', *Academic Radiology*, Vol. 14, No. 2, pp.207–218.

Meaney, P.M., Paulsen, K.D., Hartov, A. and Crane R.K. (1995) 'An active microwave imaging system for reconstruction of 2-D electrical property distributions', *IEEE* Trans*. on Biomed. Eng.*, Vol. 42, No. 10, pp.1017–1026.

Ostadrahimi, M., Noghanian, S. and Shafai, L. (2009) 'A modified double layer tapered slot antenna with improved cross polarization'. Paper presented at *13th International Symposium on Antenna Technology and Applied Electromagnetics (ANTEM)*, 15–18 February 2009, Banff, Canada.

Pozar, D.P. (1999) *Microwave Engineering*, John Wiley and Sons Inc.

Semenov, S., (2009) 'Microwave tomography: review of the progress towards clinical applications', *Philosophical Trans. of Royal Society on Mathematical, Physical & Engineeing Sciences*, Vol. 367, pp.3021–3042.

Sill, J. and Fear, E.C. (2005) 'Tissue sensing adaptive radar for breast cancer detection – experimental investigation of simple tumor models', *IEEE Trans. on Mic. Theory and Tech.*, Vol. 53, No. 11, pp.3312–3319.

Winters, D.W., Shea, J.D., Madsen, E.L., Frank, G.R., Van Veen, B.D. and Hagness, S.C. (2008) 'Estimating the breast surface using UWB microwave monostatic backscatter measurements', *IEEE Trans. on Biomedical Engineering*, Vol. 55, pp.247–256.

Zhang, J., Fear, E.C. and Johnston, R.H. (2009) 'Cross-Vivaldi antenna for breast tumor detection', *Mic. and Opt. Tech. Lett.*, Vol. 51, No. 2, pp.275–280.